

Feed-forward Control of a Residual Water Blunting Process

V. Mureşan, M. Abrudean, M.-L. Ungureşan, T. Coloşi

Technical University of Cluj-Napoca, Cluj-Napoca, CO 400114 RO

(Tel: +40-744-420906; +40-721-260308; +40-766-466972; +40-752-083514; e-mail: Vlad.Muresan@aut.utcluj.ro; Mihai.Abrudean@aut.utcluj.ro; Mihaela.Unguresan@chem.utcluj.ro; Tiberiu.Colosi@aut.utcluj.ro).

Abstract: In this paper, a solution for the pH control of the residual water, at the overflowing point from a blunting system, is proposed. The modeling-simulation of the blunting process and of the proposed feed-forward control structure is based on the matrix of partial derivatives of the state vector, associated with Taylor series. The approached control strategy generates much better results than in the case of using a simple control structure, fact that results from the comparative simulations presented in the “Simulations Results” chapter. Also the modeling method offers the advantage of the possibility of the simulation and control of the pH value in each point from the neutralizing tank’s volume. Another singularity of this paper is the inclusion of a distributed parameter process (modeled through an equation with partial derivatives) in a control structure.

Keywords: blunting process, numerical simulation, equation with partial derivatives, matrix of partial derivatives of the state vector (Mpdx), cream of lime, feed-forward control.

1. INTRODUCTION

The treated blunting system is used to neutralize the residual water resulted from the manufacturing flow of producing seamless steel pipes in a metallurgical factory. The residual water has to be overflowed in the closest river, being necessary to respect some chemical limits in order to avoid the river’s pollution (Mureşan, 2012). The most important chemical parameter that has to be considered is the residual water pH value, value that has to be maintained between 6.5 (the minimum limit) and 7.5 (the maximum limit). Due to the high values of the disturbances that appear in the system and due to the importance of the blunting system, it is better if the pH value tends to 7 (the neutral value for the pH). In this context, an on-off control structure or a simple control structure with a single PID (Proportional-Integrator-Derivative) controller is not sufficient. The solution that was chosen to be approached in this paper is the usage of a feed-forward control structure.

In the case of the considered blunting system, the residual water, has only an acid character (the pH value smaller than 7), the neutralizer being the cream of lime (a basic solution with the pH 12). The blunting system contains four neutralizing tanks connected in series. The connection between two consecutive tanks is made at their edges in relation with their length (the tanks have a parallelepipedic form) through the connection orifices (connection points). Both the reactants (the acid residual water and the cream of lime) are introduced in the reaction in the first tank, at its edge that does not communicate with the second tank, through the corresponding pipes. This point is considered the

input point in the blunting system. The output point of the blunting system is considered the overflowing point from the tank number four. This point is at the edge of tank number four that does not communicate with the third tank.

The four tanks contain each a barbotage mix up system. The barbotage system has the purpose to accelerate the chemical reaction between the two reactants and the purpose to homogenize the pH value of the residual water in the tanks. The air, under pressure, is introduced in the lower part of the tanks through a system of pipes. Due to the barbotage system, due to the fact that between each two consecutive tanks, a difference of level exists and due to the fact that the reactants are continuously introduced in the reaction, the chemical’s circulation from the input point of the system to the output point (the overflowing point) of the system appears. In Fig. 1, the general diagram of the blunting system is presented.

The feedback signal associated to the pH controller (AC) is generated by a pH transducer that is placed at the overflowing point from the blunting system. The control signal generated by the pH controller is applied to the actuator, in this case an electro-valve installed on the cream of lime pipe, the effect being the variation of the cream of lime flow (in this case, the actuating signal). The main disturbances are the acid’s pH and the acid’s input flow. These two quantities are measured using a pH transducer and a flow transducer, both placed on the acid pipe. The feedback signal associated to the second controller (the compensation block CB) results as the product between the output signals of the two transducers (from the acid pipe), the explanations regarding this aspect being given in the following chapters.

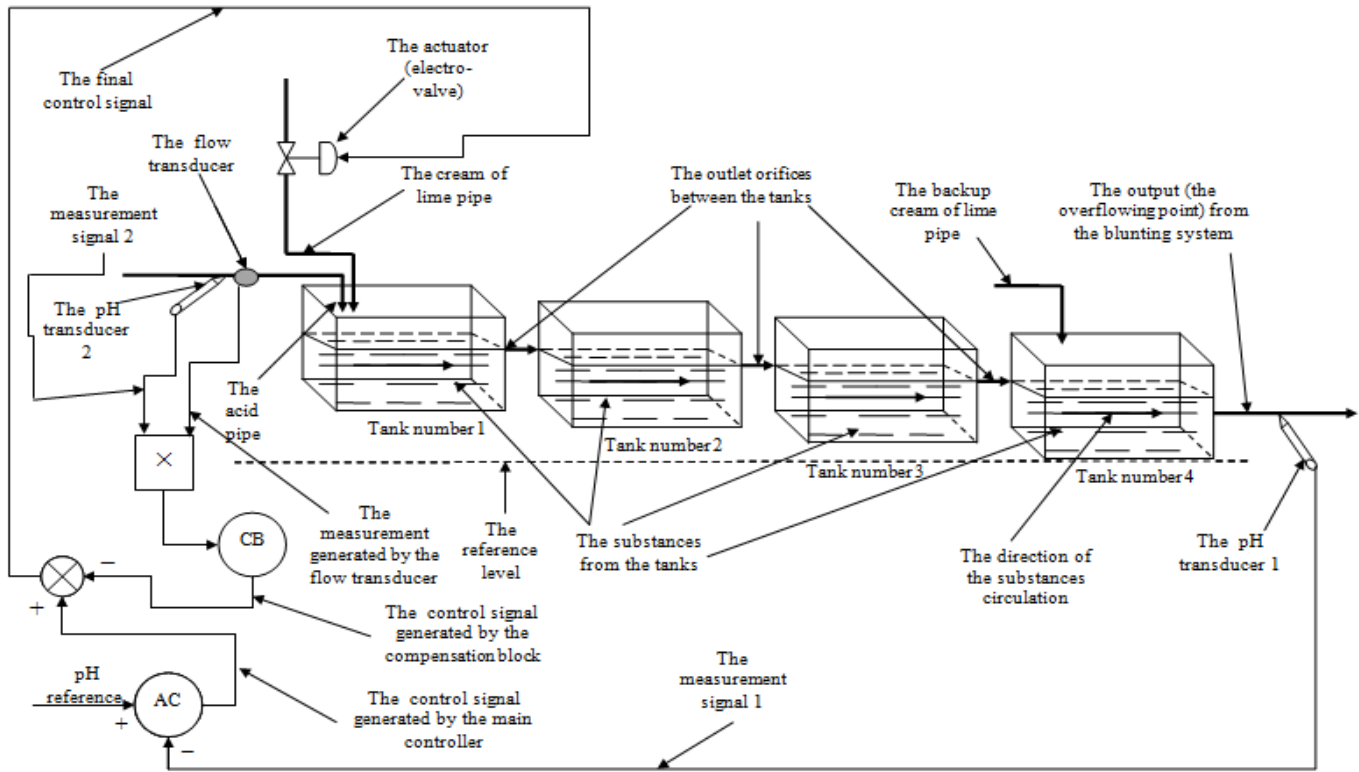


Fig. 1. The general diagram of the blunting system.

The final control signal results subtracting the control signal generated by the compensation block (Golnaraghi, 2009) from the control signal generated by the main controller (AC). The communication between the two controllers and the corresponding three transducers, respectively between the controllers and the actuator is made through unified current signals (4-20 mA).

2. MODELING OF THE BLUNTING PROCESS

The four tanks have the same technical characteristics and the same role to homogenize the chemical's pH value from the blunting system. Considering these aspects, the four tanks can be viewed and treated as an equivalent tank. Both the technical characteristics of each tank, respectively the technical characteristics of the equivalent tank are presented in the following table (Table 1).

Table 1. The technical characteristics of the tanks

The technical characteristics of the tanks	The length	The width	The depth	The volume
Tanks 1,2,3,4	5 m	2 m	1.5 m	15 m ³
The equivalent tank	20 m	2 m	1.5 m	60 m ³

Due to the circulation of the substances from the input point to the overflowing point of the blunting system, the reaction

between the two reactants appears progressively. This remark implies the fact that besides the time variable (*t*) the pH value of the chemical from tanks depends on their position in the tank, too. The blunting process, depending on more than one independent variable, is a distributed parameter one (Curtain, 2009; Li, 2011; Russell, 2010). The three independent variables (*p*), (*q*) and (*r*) that define the position in the blunting system are introduced using the Cartesian space representation, as it can be remarked from the general structure of the equivalent tank presented in Fig. 2.

The back-up cream of lime pipe from Fig. 2, is used only in failure procedures and will not be considered in the model of the process. Also, in Fig. 2, the difference of level between the input and the overflowing point of the tank is shown (the difference of level is necessary in order to maintain the same conditions as in the Fig's 1 case). The origin line is considered at the input in the system (the edge of the equivalent tank where the two reactants are introduced) at the separation limit between the chemical from the tank and the air. The origin of the Cartesian space is placed on the origin line in the center of the tank related to its width.

The pH variation on the tank's length, width and depth corresponds with the pH variation on the $0p$, $0q$, respectively $0r$ axes. The pH's value homogenization is made with a very high efficiency especially in the tank's width, respectively depth due to the barbotage system. This aspect implies the fact that the pH variation on the $0q$ and $0r$ axes have an insignificant weight comparing with the pH variation on the $0p$ axis case.

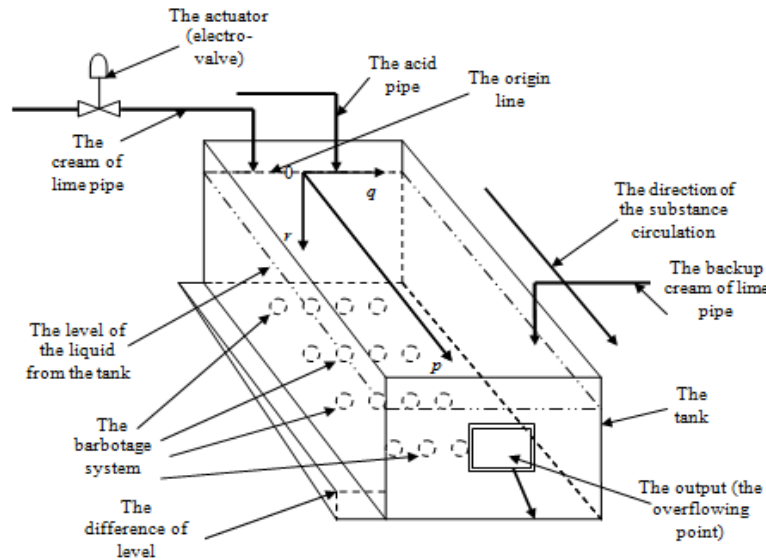


Fig. 2. The general structure of the equivalent tank.

Considering the previous remark, the conclusion is that in the model of the blunting process, only the pH variation on the $0p$ axis case is considered, more exactly besides the time independent variable (t) only the “length” independent variable (p) is considered.

The model of the distributed parameter processes can be expressed using equations with partial derivatives (PDE) (Mureşan, 2010; Krstic, 2006). In the case of the considered blunting process, its model can be expressed using an equation with partial derivatives of second order with two independent variables (time and length) (PDE II-2). If the

notation $y_{TP} = \frac{\partial^{T+P} y}{\partial t^T \partial p^P}$ is made, where $T=0,1,2,\dots$, and

$P=0,1,2,\dots$, the general form of the equation that describes the process work is presented in the following relation:

$$a_{00} \cdot y_{00} + a_{10} \cdot y_{10} + a_{01} \cdot y_{01} + a_{20} \cdot y_{20} + a_{11} \cdot y_{11} + a_{02} \cdot y_{02} = \varphi_{00} \quad (1)$$

The previous notation is valid for φ function, too. Also, in (1) the coefficients are constant and the functions $y(t,p)$ (the pH value of the chemical from the tank) and $\varphi(t,p)$ respect Cauchy conditions of continuity.

In the modeling procedure (Maga, 2011) it has to be taken in consideration the fact that in the equivalent tank, two reactants are introduced. Considering this aspect, the blunting process can be decomposed in two sub-processes. The first sub-process represents the effect of the acid introduced in the reaction upon the output signal, respectively the second sub-process represents the effect of the cream of lime introduced in the reaction upon the output signal. The output signal (the pH of the chemical at the overflowing point) of the blunting process will result as the sum between the output signals of the two sub-processes. To obtain the model of the two sub-processes, the hypothesis that the equivalent tank is full with liquid of pH value equal to 7 (the pH indifferent value) is considered. Also, in the modeling procedure, the flows of the

two reactants are considered constant and equal between them, the variation of the output signal resulting as an effect of the variation of the pH values of the two substances at the input in the process.

In Fig. 3, the block diagram of the blunting process, decomposed in two sub-processes is presented. In Fig. 3, it can be remarked that the first sub-process model is represented using PDEA, respectively the second sub-process model is represented using PDEB. Also, in Fig. 3, the input, the output and the intermediary signals are represented. Next, the modelling procedure for the two sub-processes is presented. In the first sub-process case, the acid is introduced in the tank and in the same time, through the cream of lime pipe, a liquid with the pH value equal to 7 is introduced. The input signal $u_A(t)$ has the value equal to the difference between the acid’s pH and 7. Hence, the input signal will have a negative step variation form. The effect of applying this signal at the input of the sub-process is a decreasing evolution of the value of the output signal $y_A(t,p)$ under the value of 7 (the pH indifferent value from the chemical point of view). In the second sub-process case, the cream of lime is introduced in the tank and in the same time, through the acid pipe, a liquid with the pH value equal to 7 is introduced.

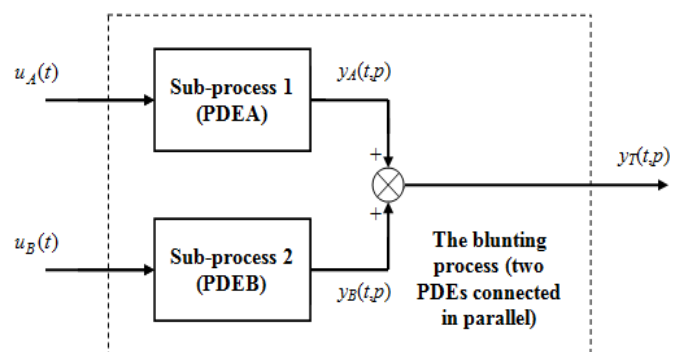


Fig. 3. The block diagram of the blunting process.

The input signal $u_B(t)$ has the value equal to the difference between the cream of lime's pH and 7. Hence, the input signal will have a positive step variation form. The effect of applying the positive step signal at the input of the second sub-process is an increasing evolution of the value of the output signal $y_B(t,p)$ over the value of 7. The model of each sub-process can be expressed using the equation from relation (1) by replacing y function with $y_A(t,p)$ ($y_{00A}(t,p)$) or $y_B(t,p)$ ($y_{00B}(t,p)$). The output signal of the blunting process associated to the equivalent tank will be the sum between the output signals from the two sub-processes:

$$y_T(t,p) = y_A(t,p) + y_B(t,p). \tag{2}$$

The $y_T(t,p)$ signal represents the pH value of the chemical from the equivalent tank if both the acid and the cream of lime are introduced through the corresponding pipes.

Only a subscript attached to the functions $u_{0A}(t)$, respectively $u_{0B}(t)$ (without considering the A and B letters that determine the sub-process) signifies the differentiation order of those elements related to the independent variable (t). This notation remains valid for the following intermediary signals presented in this paper, too.

The approximating analytical solutions that verify relation (1), for the two sub-processes are:

$$y_{00Ai}(t,p) = K_y \cdot F_{0Ti}(t) \cdot F_{0Pi}(p) \cdot u_{0i}(t) \tag{3}$$

where i can be A or B . In relation (3) K_y represents the proportionality constant of the process. K_y is a dimensionless coefficient and after some analytical calculations resulted $K_y = 0.25$. Also

$$F_{0Ti}(t) = 1 - \frac{T_1}{T_1 - T_2} \cdot e^{-\frac{t}{T_1}} - \frac{T_2}{T_2 - T_1} \cdot e^{-\frac{t}{T_2}}, \text{ and}$$

$F_{0PAi}(p) = \sigma_0 + \sigma_1 \cdot e^{-\frac{p}{P_1}} + \sigma_2 \cdot e^{-\frac{p}{P_2}}$. T_1 and T_2 are the time constants of the process and P_1 and P_2 can be called "the length constants" of the process. The relations of the σ coefficients will be presented later in this chapter. The analytical model was approximated using some intermediary representative measurements from the process. The measurements are based on the step response of the process. The experimental curves are obtained measuring the evolutions in time of the pH value in different points from lengths of the tanks from the system (including the input point in the system, some intermediary points and the overflowing point from the system).

After accomplishing the necessary experiments on the plant, it results that the speed of the chemical reaction decreases with the length increasing on the $0p$ axis. The effect of this remark is that the value of the time constants T_1 and T_2 differs for different points on the $0p$ axis. Hence, higher the value of the distance from the origin of the Cartesian system

on the $0p$ axis is, higher the values of the time constants are. The evolution of the analytical solution of the equation from relation (1) singularized for the sub-process A, related to the two independent variables (t and p), $u_A(t)$ being a negative step signal, is qualitatively presented in Fig. 4. Also, the evolution of the analytical solution of the equation from relation (1) singularized for the sub-process B, related to the two independent variables (t and p), $u_B(t)$ being a positive step signal, is qualitatively presented in Fig. 5.

In Figs. 4 and 5, the indexes 0 signify the initial values, i indexes signify the initial values too, f indexes signify the final values, respectively indexes α and β signify the difference between the settling time of the response for p_0 and for p_f . On the origin line, the reaction does not occur, the value of the response remaining constant at the value 7 (y_i). In the immediate neighbourhood of the origin (p_0), the reaction occurs very fast but the pH value (for $t_{f\alpha}$) remains near 7 (y_i) because the reaction is only at the start. At the overflowing point (p_f) the reaction appears slower but the pH value (for $t_{f\beta}$) presents a maximum variation in relation to (y_i) because the reaction is complete.

From Fig. 4 and Fig. 5, results the antagonistic effect of the acid, respectively of the cream of lime introduced in the process. Making the sum of the two effects and considering the appropriate values of the flows of the two substances, the resultant will become null creating the possibility to control (Inoan, 2010) the pH value.

The time constants were identified using the tangent method (Abrudean, 1998), resulting the values $T_{1\alpha} = 2.56$ min and $T_{2\alpha} = 3.84$ min for $y(t, p_0)$, respectively $T_{1\beta} = 7.04$ min and $T_{2\beta} = 10.56$ min for $y(t, p_f)$. The evolution of the time constants from p_0 to p_f is approximately linear and is

$$\text{given by the relations: } T_{1\gamma} = \frac{T_{1\beta} - T_{1\alpha}}{p_f - p_0} \cdot p, \quad T_{2\gamma} = \frac{T_{2\beta} - T_{2\alpha}}{p_f - p_0} \cdot p$$

where $p_0 \leq p \leq p_f$ and $t_\alpha \leq t_\gamma \leq t_\beta$. "The length constants" of the process were identified using a method based on an interpolation procedure, resulting the values $P_1 = 1.6$ m and $P_2 = 2.4$ m. Using these values, the $a...$ coefficients from relation (1) can be calculated with the next formulae: $a_{00} = 1$, $a_{10} = T_{1\gamma} + T_{2\gamma}$, $a_{20} = T_{1\gamma} \cdot T_{2\gamma}$, $a_{01} = P_1 + P_2$, $a_{02} = P_1 \cdot P_2$ and $a_{11} = (T_{1\gamma} + T_{2\gamma}) \cdot (P_1 + P_2)$. Also σ coefficients from the relations of $F_{0Pi}(p)$ can be calculated with the following formulae:

$$\sigma_{0i} = \frac{y_{fi}}{u_{0i}}, \quad \sigma_{1i} = \frac{y(t_{fai}, p_0) - y_{fi}}{u_{0i}} \cdot \frac{P_1}{P_1 - P_2}, \quad \text{respectively}$$

$$\sigma_{2i} = \frac{y(t_{fai}, p_0) - y_{fi}}{u_{0i}} \cdot \frac{P_2}{P_2 - P_1} \quad \text{where } i \in \{A, B\}. \quad \text{The}$$

identified time and length constants, being structure parameters, remain the same for both two sub-processes.

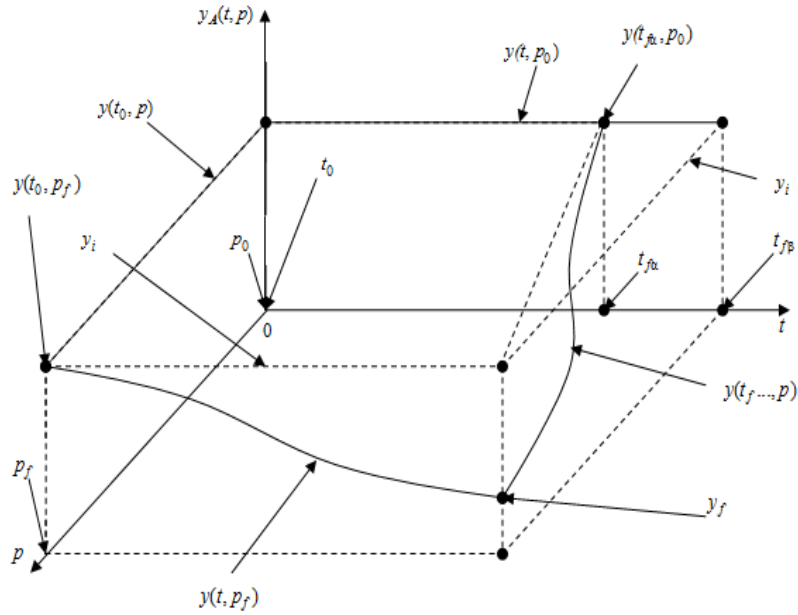


Fig. 4. The evolution of the analytical solution related to t and p , for the sub-process A.

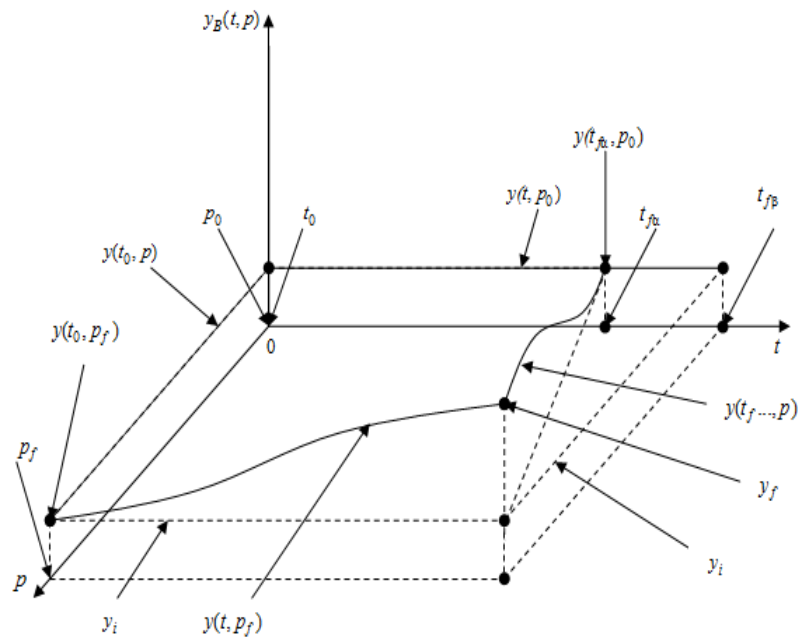


Fig. 5. The evolution of the analytical solution related to t and p , for the sub-processes B.

3. MODELING AND SIMULATION OF THE pH CONTROL SYSTEM

The feed-forward control structure for the pH control is presented in Fig. 6. The significance of the new notations from Fig. 6 is: AC—the main pH controller of PID type (Love, 2007); CB—the second controller (the compensation block); A—actuator (the electro-valve); MT1, MT2—pH transducers; MT3—the flow transducer; $a(t)=a_0$ —error signal; $ca(t)=ca_0$ —the control signal generated by the main pH controller; $cb(t)=cb_0$ —the control signal generated by the compensation

block (the second controller); $cf(t)=cf_0$ —the final control signal applied to the actuator; $w(t)=w_0$ —the reference signal; $f(t)=f_0$ —the actuating signal, representing the flow of the cream of lime, after the actuation generated by the controllers; $mT(t)=mT_0$ —the measurement signal generated by the pH transducer placed at the overflowing point from the equivalent tank, $mA(t)=mA_0$ —the measurement signal generated by the pH transducer placed on the input acid pipe; $mF(t)=mF_0$ —the measurement signal generated by the flow transducer placed on the input acid pipe. K_{pH} represents a proportionality constant equal to 5 (pH of cream of lime – 7).

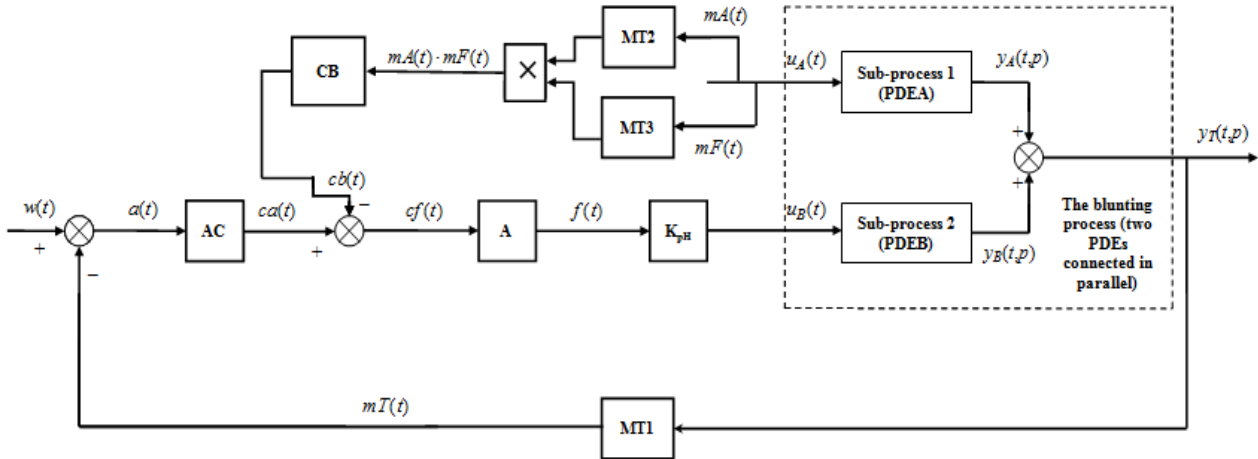


Fig. 6. The feed-forward control structure.

In the case of the control structure, $u_A(t)$ and $u_B(t)$ represent the product between the flow of the two reactants and the values of the differences between their pH and 7. Hence, $u_{0A}(t) = F_A(t) \cdot (\text{pH}_A(t) - 7)$, respectively $u_{0B}(t) = F_B(t) \cdot K_{\text{pH}}$, where $F_A(t)$ is the input flow of the acid, $F_B(t)$ is the input flow of the cream of lime and $\text{pH}_A(t)$ is the input pH of the acid. In the control structure (Miron, 2010; Sita, 2012), the effect of the acid reactant (the output of PDEA) can be viewed as a disturbance signal (Teppa-Garran, 2013). But this effect is given by both $F_A(t)$ and $\text{pH}_A(t)$ signals, these being considered the disturbance signals. Reductively, the feedback from the disturbance will result measuring the $F_A(t)$ and $\text{pH}_A(t)$ signals. The analogue modeling of the system presented in Fig. 6 starts from the following system of equations:

$$\text{Transducer 1: } \begin{cases} mT_0 \\ mT_1 = \frac{1}{T_T} \cdot [K_T \cdot (y_{00A} + y_{00B}) - mT_0] \end{cases} \quad (4)$$

$$\text{Transducer 2: } \begin{cases} mA_0 \\ mA_1 = \frac{1}{T_T} \cdot [K_T \cdot \text{pH}_{0A} - mA_0] \end{cases} \quad (5)$$

$$\text{Transducer 3: } \begin{cases} mF_0 \\ mF_1 = \frac{1}{T_{TF}} \cdot [K_{TF} \cdot D_{0A} - mF_0] \end{cases} \quad (6)$$

The main PID controller (AC):

$$\begin{cases} ca_0 \\ ca_1 = \frac{1}{T_R} \cdot [K_{PR} \cdot (w_0 - mT_0) + K_{DR} \cdot (w_1 - mT_1) - ca_0] \\ ca_2 = \frac{1}{T_R} \cdot [K_{PR} \cdot (w_1 - mT_1) + K_{IR} \cdot (w_0 - mT_0) + \\ + K_{DR} \cdot (w_2 - mT_2) - ca_1] \end{cases} \quad (7)$$

The second controller (the compensation block) (CB):

$$\begin{cases} cb_0 \\ cb_1 = \frac{1}{T_{RC}} \cdot [K_{PRC} \cdot (mA_0 \cdot mF_0) + \\ + K_{DRC} \cdot (mA_1 \cdot mF_0 + mA_0 \cdot mF_1) - cb_0] \\ cb_2 = \frac{1}{T_{RC}} \cdot [K_{PRC} \cdot (mA_1 \cdot mF_0 + mA_0 \cdot mF_1) + \\ + K_{IRC} \cdot (mA_0 \cdot mF_0) + \\ + K_{DRC} \cdot (mA_2 \cdot mF_0 + 2 \cdot mA_1 \cdot mF_1 + mA_0 \cdot mF_2) - cb_1] \end{cases} \quad (8)$$

The final control signal:

$$cf_0 = ca_0 - cb_0. \quad (9)$$

$$\text{Actuator: } \begin{cases} u_{0B} \\ u_{1B} = \frac{1}{T_{EE}} \cdot (K_{\text{pH}} \cdot K_{EE} \cdot cf_0 - u_{0B}) \end{cases} \quad (10)$$

Sub-processes 1 and 2 ($i \in \{A, B\}$) (PDE II·2):

$$\begin{cases} y_{00i} \\ y_{10i} \\ y_{20i} = \frac{1}{a_{20}} \cdot [\varphi_{00i} - (a_{00} \cdot y_{00i} + a_{10} \cdot y_{10i} + \\ + a_{01} \cdot y_{01i} + a_{11} \cdot y_{11i} + a_{02} \cdot y_{02i})] \end{cases} \quad (11)$$

In the previous relations, the following symbols have also been used: K_T – the proportionality constant of the pH transducers, T_T – the time constant of the pH transducers (the two pH transducers are of the same type), K_{TF} – the proportionality constant of the flow transducers, T_{TF} – the time constant of the flow transducers, K_{PR} – the proportionality constant of the main controller (AC), K_{IR} – the integrative constant of the main controller (AC),

K_{DR} —the derivative constant of the main controller (AC), T_R —the inertial time constant of the main controller (AC), K_{PRC} —the proportionality constant of the compensation block (CB), K_{IRC} —the integrative constant of the compensation block (CB), K_{DRC} —the derivative constant of the compensation block (CB), T_{RC} —the inertial time constant of the compensation block (CB) K_{EE} —proportionality constant of the actuator and T_{EE} —the time constant of the actuator. In (8), the extended terms from the round brackets resulted from the first, respectively from the secondary differentiation of the term ($mA_0 \cdot mF_0$).

The elements of the state vector \mathbf{x}_B associated to the control system, presented in transposed form in (12) are obtained from the relations (4)-(8) and (10)), respectively the elements of the state vector \mathbf{x}_A associated to the sub-process 1 (PDEA), presented in transposed form in (13) are obtained from the relation (11).

$$\mathbf{x}_B^T = \begin{bmatrix} mI_0 & mI_1 & mA_0 & mA_1 & mF_0 & mF_1 & ca_0 & ca_1 & cb_0 & cb_1 & u_{0F} & u_{1F} & y_{00F} & y_{10F} \end{bmatrix} \quad (12)$$

$$\mathbf{x}_A^T = \begin{bmatrix} y_{00A} & y_{10A} \end{bmatrix} \quad (13)$$

Considering the values $M=8$ and $N=35$, respectively $M=8$ and $N=5$ definitive for the dimension of matrices \mathbf{M}_{pdxB} and \mathbf{M}_{pdxA} (the matrix of partial derivatives of the state vector), these are presented in relations (14) and (15) [Coloși T., 2013].

$$\mathbf{M}_{pdxB} = \begin{matrix} \begin{matrix} \xrightarrow{1} & \xrightarrow{M=8} \\ \begin{bmatrix} \mathbf{x}_B & \mathbf{x}_{EB} \\ \mathbf{x}_{TB} & \mathbf{x}_{TEB} \end{bmatrix} & \begin{matrix} \uparrow n=14 \\ \downarrow N=35 \end{matrix} \end{matrix} \end{matrix} \quad (14)$$

$$\mathbf{M}_{pdxA} = \begin{matrix} \begin{matrix} \xrightarrow{1} & \xrightarrow{M=8} \\ \begin{bmatrix} \mathbf{x}_A & \mathbf{x}_{EA} \\ \mathbf{x}_{TA} & \mathbf{x}_{TEA} \end{bmatrix} & \begin{matrix} \uparrow n=2 \\ \downarrow N=5 \end{matrix} \end{matrix} \end{matrix} \quad (15)$$

The matrices and vectors that occur in relations (14) and (15) are: the state vector \mathbf{x}_i ; the vector of partial derivatives related to time (t) of the state vector \mathbf{x}_{Ti} ; the matrix of partial derivatives related to independent variable (p) of the state vector \mathbf{x}_{pi} ; the matrix of partial derivatives related to time (t) and to the independent variable (p) of the state vector \mathbf{x}_{TPi} ; i can be A or B . Thus, it results that the matrices \mathbf{M}_{pdxB} and \mathbf{M}_{pdxA} have the dimensions (\mathbf{M}_{pdxB} (49·9)), respectively (\mathbf{M}_{pdxA} (7·9)).

To start the numerical simulation, the initial conditions of the elements of the two \mathbf{M}_{pdx} matrices are needed to be known or calculated. A possibility to calculate them is to use the analytical solution of the two sub-processes. After doing the calculations, we can make the matrices (\mathbf{M}_{pdx_i}) ($i \in \{A, B\}$) for the initial conditions ($(\mathbf{M}_{pdx_i})_{IC}$) that correspond to the start sequence ($k-1$). In order to advance from sequence ($k-1$) to sequence (k) we need to use the Taylor series (Coloși, 2013). The numerical simulation is finished when $t \geq t_{f\beta}$ (final simulation time β). In all the relations from this section we considered that the integration step (Δt) has a value that is small enough, so that the numerical integration is being done correctly. For the case of blunting process composed of two sub-processes, the relation (2) can be applied to obtain the process output.

4. THE SIMULATIONS RESULTS

The simulation applications were developed in MATLAB environment (User Guide). After simulation, the comparison between the response that resulted through numerical integration and the analytical response of the system was made, through the calculus of the cumulated relative error in percentage (Ungureșan, 2011). The simulations were made for the case of continuous functioning.

The main controller's parameters (AC): $K_{PR} = 9.6$, $K_{IR} = 0.5455 \text{min}^{-1}$ and $K_{DR} = 40.5504 \text{min}$ were obtained using an adapted form of the module criterion for PDEs. The compensation block (CB) was tuned using the classical method for feed-forward control systems considering the inertia of the elements from the secondary loop associated to the disturbance signal. After calculus, the following parameters resulted: $K_{PRC} = 2.6667$, $K_{IRC} = 0 \text{min}^{-1}$ and $K_{DRC} = 11.2640 \text{min}$. It can be remarked that the main controller is of PID type and the compensation block is of PD type.

In Fig. 7 the comparative graph between the analytical and the numerical response of the automatic control system is presented (the variation in time of the $y_T(t,p)$ signal – the pH value of the chemical at the overflowing point from the equivalent tank). The reference signal's value was fixed at 7 (the indifferent pH value) and the disturbance signal was generated from the PDEA's input step type signal: $u_{0A}(t) = F_A(t) \cdot (\text{pH}_A - 7)$, where the acid's flow $F_A(t) = \text{const.} = 31 / \text{s}$ and the acid's pH $\text{pH}_A = \text{const.} = 3$. The previous relation shows that the value of the first sub-process output signal can be modified either through the value of $F_A(t)$ or the value of pH_A . In the tank, at the initial moment, the value 7 for the chemical's pH was considered. Also this simulation is made at the overflowing point ($p = p_f$) from the equivalent tank.

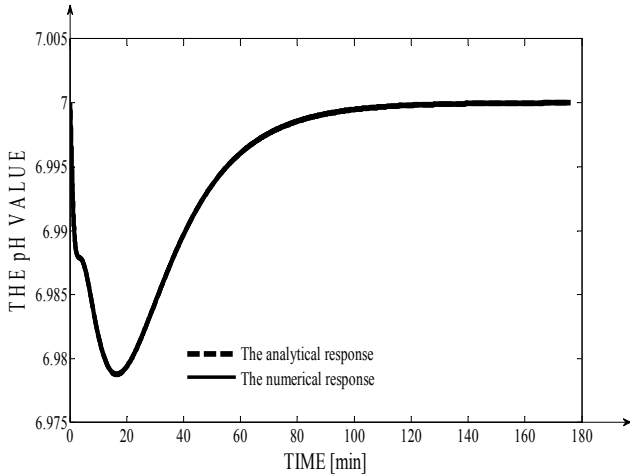


Fig. 7. The comparative graph between the analytical and the numerical response of the process for $p = p_f$.

In Fig. 7, it can be remarked that the value of the overshoot is $\sigma = -0.3\%$ (value smaller in module than the imposed one: -7%) and the value of the steady state error at position $a_{stp} = 0$ (the imposed value). Practically, the system “remains” in steady state regime because the response is enclosed into the stationary band of $\pm 3\%$ near 7, introducing the possibility that the value of the settling time to be considered 0. The very good performances of the control system is due to the action of the compensation block that forces the input of a high quantity of cream of lime in the moment when the disturbance appears (in this case at the start of the simulation). Practically, the effect of the disturbance is rejected “almost” in the same time with its propagation. Very important in this case, is the derivative component of the CB element.

On Fig. 7, we cannot differentiate the two responses due to the very small error between them. The variation in time of the cumulative error in percentage is presented in Fig. 8. The maximum value of the error is $2.5 \cdot 10^{-5}\%$ right at the beginning of the numerical simulation. This maximum is due to the fact that the pH value presents in this domain a high variation in relation to time, implying high values for the derivatives in relation to time.

After the first integration steps, the value of the error decreases and, in steady state regime, it remains constant, approximately to $4.44 \cdot 10^{-6}\%$. These very low values (near 0) show the very good performances of the numerical simulation method.

The actuating signal ($f(t)$) simulated through numerical integration is presented in Fig. 9. From Fig. 9, it results that the maximum and also the steady state value of the actuating signal is 2.4 l/s, value smaller than the saturation limit (4 l/s). Also a very important aspect is that the actuating signal does not present value jumps.

Another advantage of the numerical simulation method is the fact that the user can have access to the intermediary values.

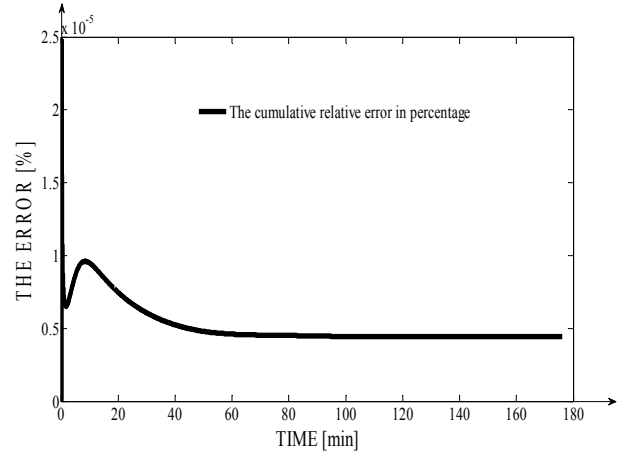


Fig. 8. The cumulative relative error in percentage between the analytical and the numerical response.

In Fig. 10 is taken the example of the control signal generated by the main pH controller, of the final control signal and of the error signal. The variation of these signals is presented considering the 0 value (4mA) for the unified current signals (4-20mA).

From Fig. 10, results the fact that the control signals have lower values than the saturation limit (20mA). Also, the error signal, in steady state regime, tends to the value 0, showing that the pH value at the overflowing point from the equivalent tank is the imposed one.

In Fig. 11, the comparative graph between the numerical response of the automatic control system in the case of using the feed-forward control structure (the previous presented case) and the numerical response in the case of using a simple structure (with only one pH transducer placed at the overflowing point from the blunting system) are presented.

From Fig. 11 we can remark the fact that the performances obtained in the case of using the feed-forward structure are much more superior than in the case of using the simple structure.

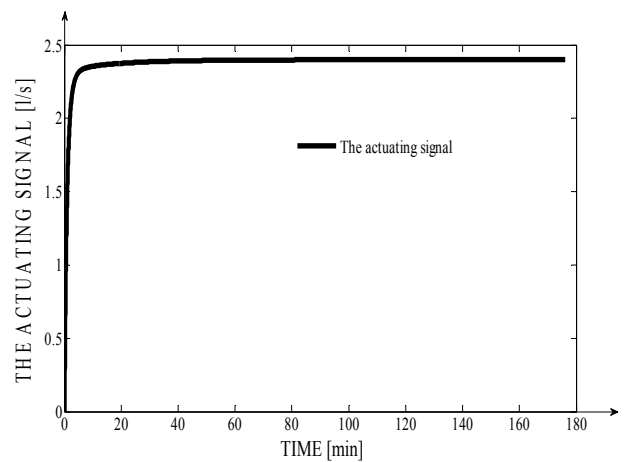


Fig. 9. The actuating signal simulated through numerical integration.

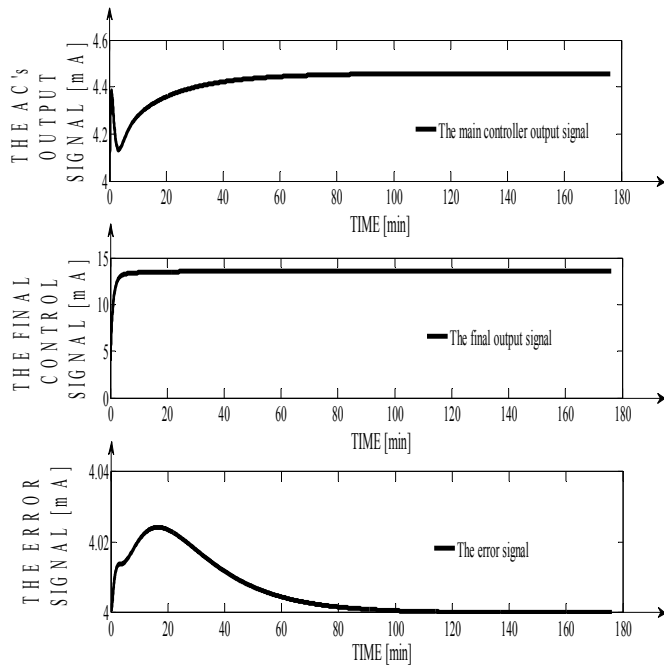


Fig. 10. The intermediary signals simulated through numerical integration.

This simulation was made for the best controller that could be obtained for the simple control structure ($K_{PR} = 8.2286$, $K_{IR} = 0.4675\text{min}^{-1}$ and $K_{DR} = 34.7575\text{min}$), the corresponding performances being $\sigma = -6.65\%$ ($|-6.65\%| \gg |-0.3\%|$), the settling time is $t_r = 64\text{min}$ (in the case of the feed-forward structure the settling time can be considered 0 min) and the value of the steady state error at position $a_{stp} = 0$ (in both cases). Also, the minimum value of the response of the simple control structure is very close to the minimum limit of 6.5, fact that has to be avoided in order to assure the safety in working.

A very important aspect is the study of the feed-forward control structure when the two disturbances $F_A(t)$ and $\text{pH}_A(t)$ are more severe than in the previous case.

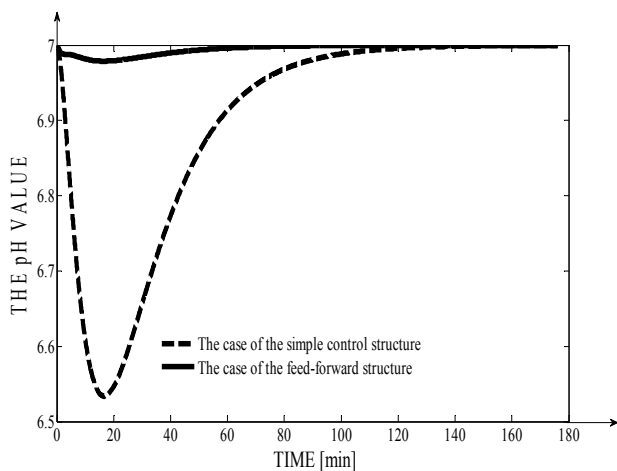


Fig. 11. The comparative graph between the cases of using the feed-forward and the simple control structure.

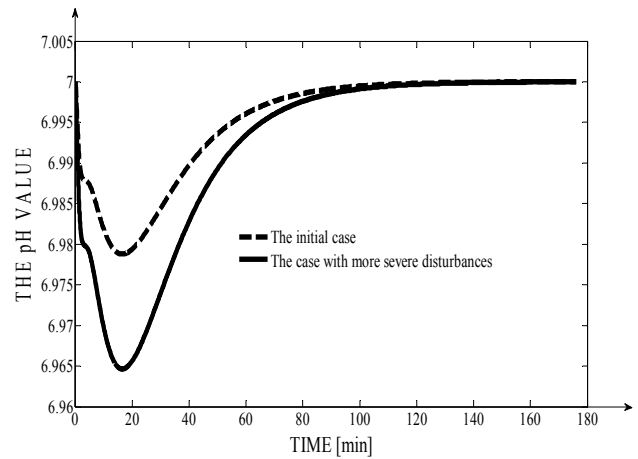


Fig. 12. The comparative graph between the initial case and the case of introducing more severe disturbances.

In Fig 12 are presented a comparative graph between the system's response for the initial case (case of Fig. 7; in Fig 12 with dashed line) and the system's response if $F_A(t) = \text{const.} = 4\text{l/s}$ and $\text{pH}_A = \text{const.} = 2$ (in Fig. 12 with continuous line).

In Fig. 12, it can be remarked that the effect of the disturbance is rejected (the steady state value of the system's response is 7). The main difference between the two cases is the value of the overshoot $\sigma_1 = -0.5\%$ in the case of considering more severe working conditions. However, this difference is insignificant in the analysis of the control system's performances. The conclusion of the simulation from Fig. 12 is the fact that the feed-forward control structure is very efficient and it generates very good results (performances).

5. CONCLUSIONS

1. The paper proposes a feed-forward control strategy for the pH control in a residual water blunting system. The modeling-simulation method, for the automatic control system of the blunting process, used for the presented application is based on the matrix of the partial derivatives of the state vector (M_{px}), associated with Taylor series, method that assures a very high accuracy of the numerical simulation.
2. The very high accuracy is demonstrated by the fact that the cumulative relative error in percentage calculated between the analytical and the numerical response of the process has very small values (near to 0). The error was presented only for the simulation from Fig. 7, but the obtained errors from all the simulation from this paper have approximately the same values as in the mentioned case.
3. The value of the integration step used for the numerical simulation is $\Delta t = 0.01\text{min}$, an appropriate value for this application.
4. The procedure of decomposing the process in two sub-processes connected in parallel has very big advantages in the implementation of the pH automatic control system because

the effects of the two reactants on the output signal can be separated. Practically, the purpose of the control structure, in the context of a blunting system, is the annulment of the two antagonistic effects introduced by two reactants (an acid and a base).

5. Although the input signals in the sub-processes are products between the reactants flows, respectively the reactants pH, we use the simplifier hypothesis that these do not introduce non-linearity (Godasia, 2002) in their models, due to the big volume of the tanks.

6. The two sub-processes from the structure of the blunting process are viewed as processes with distributed parameters and are modeled through equations with partial derivatives. This approach permits the pH control in different points on the tanks lengths.

7. All the imposed performances to the control system were respected. Also, in the simulation from Fig. 11, it was shown the fact that the feed-forward control structure generates very good results comparing with the simple control structure, its implementation being justified.

8. In the control structure, the two main disturbances are considered (the acid's pH and the acid's flow), being assured the feedback in relation with the both mentioned signals. The resulted measurement signals are operated after a PD control law by the second controller (the compensation block – CB).

REFERENCES

- Abrudean, M. (1998). *Systems theory and automatic regulation*. 170 Pages. MEDIAMIRA Publishing house, Cluj-Napoca.
- Coloși T., Abrudean M., Ungureșan M.-L. and Mureșan V. (2013). *Numerical Simulation of Distributed Parameters Processes*. 363 pages. SPRINGER Publishing house.
- Curtain R.F. and Morris K.A. (2009). Transfer Functions of Distributed Parameter Systems. *Automatica*, 45, 5, pp. 1101-1116.
- Godasia S., Karakasb A. and Palazoglu A. (2002). Control of nonlinear distributed parameter processes using symmetry groups and invariance conditions. *Computers & Chemical Engineering*, 26, 7-8, pp. 1023-1036.
- Golnaraghi F. and Kuo. B. C. (2009). *Automatic Control Systems*. 786 pages. Wiley Publishing house.
- Inoan I. (2010). Movement control of an unloading machine from a rotary furnace. *Proc. of AQTR 2010, THETA 17th edition*, Cluj-Napoca, România, pp. 131-134.
- Krstic M. (2006). Systematization of approaches to adaptive boundary control of PDEs. *International Journal of Robust and Nonlinear Control*, vol. 16, pp. 801-818.
- Li H.-X. and Qi. C. (2011). *Spatio-Temporal Modeling of Nonlinear Distributed Parameter Systems: A Time/Space Separation Based Approach*. 194 pages. 1st Edition. Springer Publishing house.
- Love J. (2007). *Process Automation Handbook*. 1200 pages. Springer Publishing house.
- Maga C.R. and Jazdi N. (2011). Survey, Approach and Examples of Modeling Variants in Industrial Automation. *Journal of Control Engineering and Applied Informatics (CEAI Journal)*, 13, 1, 54-61.
- Miron R. and Leția T. (2010). Fuzzy Logic Decision in Partial Fingerprint Recognition. *AQTR 2010-THETA 17th edition*, Cluj-Napoca, Romania, Tome III pp. 439-444.
- Mureșan V. and Abrudean M. (2010). Temperature Modelling and Simulation in the Furnace with Rotary Hearth. *Proc. of 2010 IEEE AQTR 2010-17th edition*, Cluj-Napoca, Romania, pp. 147-152.
- Mureșan V., Abrudean M., Ungureșan M.-L. and Coloși T. (2012). Control of the Blunting Process of the Residual Water from a Foundry. *SACI IEEE 7th International Symposium on Applied Computational Intelligence and Informatics*, Timișoara, Romania.
- Russell D.L. (2010). Observability of Linear Distributed Parameter Systems. *The Control Handbook, Control System Advanced Methods*. Editor William Levine, CRC Press U.S.A., pp. 70-1-70-12.
- Sita I.-V. (2012). Building Control, Monitoring, Safety and Security using Collaborative Systems. *Fourth International Conference on Intelligent Networking and Collaborative Systems*, Bucharest, Romania, pp. 662-667.
- Teppa-Garran P.A. and Garcia G. (2013). Optimal Tuning of PI/PID/PID(n-1) Controllers in Active Disturbance Rejection Control. *Journal of Control Engineering and Applied Informatics (CEAI Journal)*, 15, 4, pp. 26-36.
- Ungureșan M.-L., Niac G. (2011). Pre-equilibrium Kinetics. Modeling and Simulation. *Russian Journal of Physical Chemistry*, 85, 4, pp. 549-556.
- User Guide, Matlab 7.5.0 (R2007b).